processes

MDPI

*Article*

# Research on Bolt Loosening Detection Based on Fractional Fourier Transform and Vibro-Acoustic Modulation Method

**Xiaogang Wang [1,2], Hai Yang [1,2], Jingjing Qi [1,2], Hao Zhang [1,2], Ning Zhao [1,2], Qilin Jiang [3,*] and Ning Li [3,*]**

[1] Sinopec (Shandong) Test, Evaluation & Research Co., Ltd., Dongying 257062, China; wangxg66694.slyt@sinopec.com (X.W.); yanghai.slyt@sinopec.com (H.Y.); qijingjing533.slyt@sinopec.com (J.Q.); zhanghao372.slyt@sinopec.com (H.Z.); zhaoning.slyt@sinopec.com (N.Z.)
[2] Shengli Oilfield Branch Technical Testing Center, Dongying 257062, China
[3] School of Mechanical Engineering, Yangtze University, Jingzhou 434023, China
* Correspondence: jiangqilin1029@163.com (Q.J.); lining@yangtzeu.edu.cn (N.L.)

## Abstract

By applying nonlinear vibration-to-sound modulation technology to bolt loosening detection, this paper proposes a new experimental setup and signal-processing method. A linear swept-frequency signal is used to excite low-frequency vibrations, while a fixed-frequency sine wave is used for high-frequency ultrasonic excitation. First, a fractional Fourier transform is applied to the vibration-acoustic modulation signal to transform it into the optimal fractional domain where the energy of the swept-frequency signal is concentrated; next, the swept-frequency signal undergoes a masking filter, and the filtered signal is transformed back to the time domain; finally, the time-domain signal is transformed back to the frequency domain, and the amplitudes of the sum and difference frequency components of the high-frequency signal are extracted as damage parameters. The effectiveness of this method in bolt loosening detection was verified through bolt connection tests, with the applied tightening torque ranging from 10 to 30 N·m. This method is simple to operate and highly robust, making it a reliable approach for detecting the degree of loosening in bolt connections.

**Keywords:** bolt loosening detection; vibro-acoustic modulation method; fractional Fourier transform; swept-sine wave; piezoceramic transducer

## 1. Introduction

Bolt connection, as an important fastening method for structural components, has the advantages of high strength, convenient installation, and a wide application range [1,2], and has been widely used in important industrial fields such as bridge construction, engineering equipment, and pipeline transportation. To maintain sufficient strength, rigidity, and sealing performance of the connected structural components, it is usually necessary to apply an appropriate preload to the bolts for the purpose of preventing the loosening and slipping of the bolts. However, under the influence of factors such as alternating working loads, impact loads, and changes in environmental temperature, bolt connections will inevitably experience phenomena such as material creep, stress relaxation, and fatigue crack initiation, resulting in a reduction in preload and bolt loosening. The loosening of bolts may lead to the separation of connected components or high-pressure leakage, thereby causing serious safety accidents. Therefore, conducting research on bolt connection

Check for updates

Academic Editor: Fábio Fernandes

Received: 2 March 2026
Revised: 30 March 2026
Accepted: 30 March 2026
Published: 31 March 2026

**Copyright:** © 2026 by the authors. Licensee MDPI, Basel, Switzerland. This article is an open access article distributed under the terms and conditions of the Creative Commons Attribution (CC BY) license.

loosening detection technology is conducive to ensuring engineering safety and optimizing equipment maintenance, which has significant engineering significance [3–7].

Common methods for detecting loosened bolted connections are typically divided into two main categories. One category consists of manual inspection methods, primarily including percussion testing, marking, and magnetic adhesion testing [8–10]. These methods are inefficient, costly, and lack high detection accuracy. The other category comprises non-destructive testing methods, which can be divided into two parallel technical approaches based on their underlying principles: data-driven methods and physics-model-driven methods. Data-driven methods rely on massive amounts of monitoring data and deep learning algorithms to achieve intelligent identification of loosening conditions. They primarily include automatic feature extraction and classification methods based on convolutional neural networks (CNNs), recurrent neural networks (RNNs), and their variants (such as LSTMs and GRUs) [11–13]. These methods do not require the explicit establishment of physical models and can uncover nonlinear mapping relationships within high-dimensional data, demonstrating strong adaptability under complex operating conditions. However, their performance is highly dependent on the quality and quantity of labeled data, and the models lack interpretability, making it difficult to elucidate the physical mechanisms of damage.

Physics-based methods primarily include vibration detection, mechanical impedance, acoustic emission, and ultrasonic methods [14–20]. Vibration detection is susceptible to interference from environmental noise, making quantitative analysis difficult. Mechanical impedance is significantly affected by ambient temperature and involves high detection costs. Acoustic emission signals can easily be confused with corrosion and crack damage features; this method is significantly affected by noise and is costly to implement. Ultrasonic methods are robust, simple to operate, and cost-effective. Based on the different features extracted, ultrasonic methods for detecting bolt loosening can be classified into linear ultrasonic methods [21,22] and nonlinear ultrasonic methods [23]. Among these, vibro-acoustic modulation (VAM) technology [24,25], as a contact-based nonlinear ultrasonic testing method, offers advantages such as high sensitivity to structural contact defects and strong robustness, and is attracting increasing attention from researchers.

The detection principle of VAM with bolted connections is that low-frequency vibration waves (pump waves) and high-frequency ultrasonic waves (detection waves) interact with the contact surface, causing nonlinear coupling of the two sound waves. In terms of the selection of pump waves, scholars have adopted different schemes. Parsons [26] proposes a test method based on surface-mounted piezoelectric sheets. Two excitation signals of different frequencies were generated through PZTs adhered to the surface of the structure, and the test results proved the effectiveness of this method. The method proposed by Zhao [27] uses the piezoelectric sensor PZT to generate low-frequency signals and takes the amplitude of the side lobe as the damage index to detect the magnitude of the bolt preload. WANG [28] employs a linear swept-sine signal for low-frequency and high-frequency excitation, which avoids prior understanding of the structure. The above research shows that the method of using a linear sweep frequency signal as the excitation pump signal can directly cover the potential resonance frequency band through wideband excitation without the need to predict the natural frequency parameters and is very suitable for the detection of loose bolt connections.

A linear frequency modulation (LFM) signal is a kind of non-stationary signal whose frequency changes linearly with time and has strong coupling in the time–frequency domain. It is difficult to achieve the separation of its signal and noise by using conventional time–frequency analysis methods. Fractional Fourier transform (FrFT) [29–31] is a generalized form of the Fourier transform, with chirp basis decomposition characteristics, and is a linear transformation, which is very suitable for LFM signal filtering [32,33].

This paper proposes a new method for detecting bolt connection looseness based on the vibro-acoustic modulation method and fractional Fourier transform filtering. Linear sweep frequency signals are used to excite low-frequency vibrations, while fixed-frequency sine waves are used for high-frequency ultrasonic excitation. Firstly, perform a fractional Fourier transform on the vibrating tone control signal to transform the signal to the optimal fractional domain that enables the sweep frequency signal to converge. Next, the swept-sine signal is masked and filtered, and the filtered signal is transformed back to the time domain. Then, the filtered signal is transformed from the time domain to the frequency domain, and the harmonic amplitudes of the high-frequency signal are extracted as damage parameters. Finally, the effectiveness of the proposed new method is verified through bolt connection experiments.

## 2. Theoretical Background

### *2.1. Principle of Bolt Loosening Detection Based on the Vibro-Acoustic Modulation Method*

In the bolt loosening detection method based on the vibration-acoustic modulation method, the low-frequency $\omega_l$ pump wave and the high-frequency $\omega_h$ detection wave are simultaneously input into the bolt-connected specimens. Due to the existence of the microscopic contact surface between the specimens connected by the bolts, as shown in Figure 1, the two excitation signals generate nonlinear coupling, and the high-frequency detection wave signal is modulated by the low-frequency pump wave signal. In the frequency domain, the response signal has modulated side frequencies, that is, on both sides of the detection wave frequency ($f_h \pm nf_l, n = 1, 2, \ldots$), side lobe signals containing the frequency components of the pump wave appear.

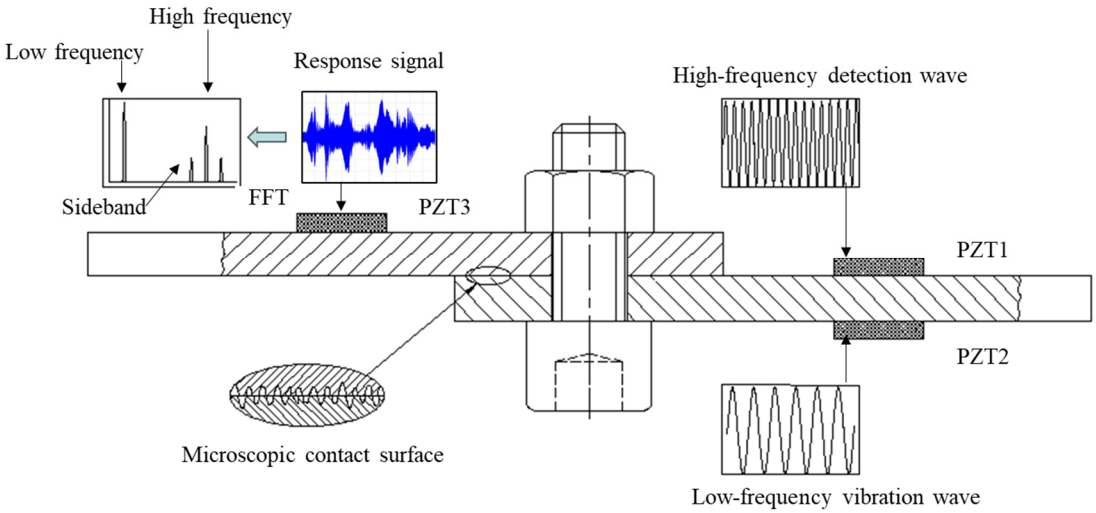



**Figure 1.** The VAM principle of bolt loosening detection.

In isotropic materials, the one-dimensional wave equation retaining the second-order nonlinear term is:

$$\frac{\partial^2 u}{\partial t^2} - c^2 \frac{\partial^2 u}{\partial x^2} = c^2 \beta \frac{\partial u}{\partial x} \frac{\partial^2 u}{\partial x^2} \tag{1}$$

In the formula, c represents the wave velocity (m/s), β is a nonlinear coefficient, u is the vibration displacement (m) of the particle, x is the propagation distance (m), and t is time.

According to the theory of micro-perturbation approximation [34], let the approximate solution of Equation (1) be:

$$u(x,t) = u_0(x,t) + \beta u_1(x,t) \tag{2}$$

In the formula: $u_0$ represents the linear displacement; $u_1$ is a nonlinear displacement.

When attenuation is not considered, the linear displacement of the vibrational tone control signal can be expressed as:

$$u_0(x,t) = A_l cos[\omega_l(t - x/c)] + A_h cos[\omega_h(t - x/c)] \tag{3}$$

In the formula: $A_l$ is the amplitude of the low-frequency pump wave and $A_h$ is the amplitude of the high-frequency detection wave.

Suppose the nonlinear displacement is:

$$u_1(x,t) = xh(t) \tag{4}$$

In the formula: h(t) is an undetermined function.

Substitute Equations (3) and (4) into Equation (2), and then substitute Equation (2) into Equation (1) to obtain:

$$\begin{aligned} u(x,t) = u_0(x,t) + \beta u_1(x,t) = A_l cos\omega_l t + A_h cos\omega_h t - \beta x\left[A_l^2 k_l^2 \cos(2\omega_l t) + A_h^2 k_h^2 \cos(2\omega_h t)\right]/8 \\ -\beta x A_l A_h k_l k_h [\cos(\omega_l - \omega_h)t - \cos(\omega_l + \omega_h)t]/4 \end{aligned} \tag{5}$$

In the formula: $k_l$ is the wave number (rad/m), $k_l = \omega_1/c$; $k_h$ is the wave number (rad/m), and $k_h = \omega_h/c$.

It can be seen from the above equation that the two signals interact with the microscopic contact surface, generating the second harmonic signal and the sum and difference frequency wave signal. The amplitude of the sidelobe signal is proportional to the nonlinear coefficient and the amplitude of the fundamental wave signal.

Let the amplitudes of the fundamental wave be $A(\omega_l) = A_l$ and $A(\omega_h) = A_h$. Under these conditions, the amplitudes of the sum and difference frequency wave signals are:

$$A(\omega_l + \omega_h) = A(\omega_l - \omega_h) = \beta x A_l A_h k_l k_h/4 \tag{6}$$

It can be seen from Equation (6) that the amplitudes of the sum and difference frequency wave signals are directly proportional to the nonlinearity coefficient, the amplitudes of the fundamental wave signals, and the frequencies of the two emitted sound waves. Therefore, the nonlinearity degree and actual contact area of the microscopic contact surface in the bolt connection structure can be evaluated based on the variation in the amplitude of the sum and difference frequency signals.

### *2.2. Principle of the Fractional Fourier Transform*

In piezoelectric ultrasonic testing, pulse waves and sweep frequency signals are two commonly used excitation methods. The pulse signal has a short duration, low emission energy, and limited propagation distance. A linear sweep frequency signal is a Chirp-based signal. If the transmission duration is long and it has a bandwidth with an adjustable frequency, it can have strong energy. The LFM signal has a large time–bandwidth product, as well as high speed resolution and distance resolution.

The fractional Fourier transform (FrFT) is a generalized Fourier transform with the decomposition characteristics of the chirp basis. FRFT can transform the signal to any intermediate domain between the time domain and the frequency domain and has a high resolution for non-stationary signals such as linear frequency modulation signals [35]. For the time-domain signal $x(t)$ and the rotation Angle θ, the FRFT result is:

$$X_\theta(u) = F^P[x(t)] = \int_{-\infty}^{\infty} x(t) K_\theta(t,u) dt \tag{7}$$

In the above equation:

$$K_\theta(t,u) = \begin{cases} \sqrt{\frac{1-jcot\theta}{2\pi}} \cdot \exp\left(j\frac{t^2+u^2}{2} \cdot cot\theta - tucsc\theta\right), & \theta \neq n\pi \\ \delta(t-u), & \theta \neq 2n\pi \\ \delta(t+u), & \theta \neq 2n(2n \pm 1)\pi \end{cases} \quad (8)$$

In the formula: $\theta = p\pi/2$ is the rotation angle of the FrFT, p is the order of the FrFT, $F^P[\cdot]$ represents the transformation operator of the FrFT, and $K_\theta(t,u)$ represents the fractional transform kernel.

By analyzing Formulas (7) and (8), it can be found that the period of the FrFT transform is 4. The FrFT can be considered as rotating the signal's coordinate axis counterclockwise by an angle theta around the origin on the time–frequency plane, transforming from the time domain t to the fractional domain u, as shown in Figure 2.

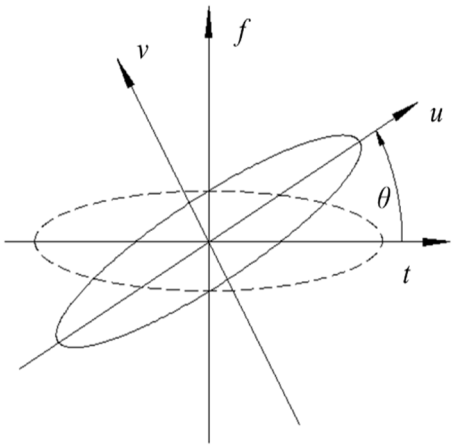



**Figure 2.** Schematic diagram of the FrFT.

By selecting an appropriate rotation angle for the FrFT transform of a linear sweep signal, the vast majority of the signal's energy can be concentrated in a specific u-domain, appearing in a form similar to the peak of an impulse function. Fixed-frequency signals and noise signals, however, will not produce similar peaks in the u-domain. Therefore, this property can be utilized to filter out the linear swept-sine signal used to excite the pump wave from the vibro-acoustic modulation signal, while retaining the high-frequency signal, modulation, and difference frequency signals used for evaluating the state of bolt connections.

### *2.3. VAM Signal-Processing Method Based on the FrFT*

Perform the FrFT on the vibration tone-modulated signal to transform the signal into the optimal fractional domain where the swept-sine signal is focused. Next, apply a bandpass filter to the swept-sine signal, and transform the filtered signal back into the time domain. Finally, transform the filtered signal from the time domain to the frequency domain, extract the amplitude of the sum and difference frequencies of the high-frequency signal, and use this as the damage parameter. The specific signal-processing steps are as follows:

(1) Apply the Hilbert transform to the bolt connection vibro-acoustic modulation signal to obtain the analytic signal of the original signal.

(2) Within the range $[0,\ 1) \cup (1,\ 2]$ for the order $p$, change the value of $p$ with a larger step size $\Delta p = 0.01$ to alter the rotation angle θ. Perform a two-dimensional scan in the FrFT plane (θ,u) and determine the fractional order $p_0$ corresponding to the peak value.

(3) In the local region centered around the value of $p_0$, specifically $[0.99p_0, 1.01p_0]$, change the value of p with a smaller step size $\Delta p$ = 0.0005 to alter the rotation angle θ. Using the FrFT, find $p^*$ and $u^*$ values corresponding to the peak point.

(4) For the peaks formed by linear frequency-sweep signals in the u domain, an ideal masking filter with center frequency $u^*$ and bandwidth $u^*/20$ is used for filtering, removing the linear frequency-sweep signals while retaining the sum and difference frequency signals and noise signals.

(5) Apply a FrFT of order -*p* to the filtered fractional domain signal and transform it back to the time domain.

(6) Perform a standard Fourier transform on the time-domain signal to obtain the amplitude spectrum diagram. Evaluate the degree of loosening of the bolt connection by transforming the sum and difference frequency amplitude values.

## 3. Experimental Setup

### *3.1. Introduction to the Bolt Loosening Detection Test Apparatus*

The VAM detection method for bolted joint conditions proposed in this paper was verified through experiments. As shown in Figure 3, the experimental setup includes two rectangular steel plates measuring 40 mm × 76 mm × 5 mm, M8 bolts (grade 8.8), nuts, a laptop, a NI DAQ 6361 data acquisition device, d33 piezoelectric ceramics with a diameter of 10 mm and a thickness of 2 mm, strong magnets with a diameter of 16 mm and a thickness of 5 mm, and an Allen wrench and a torque wrench. Two piezoelectric ceramics, PZT1 and PZT2, serve as actuators and are magnetically attached to the same steel plate; one piezoelectric ceramic, PZT3, serves as a sensor and is magnetically attached to the other steel plate. A total of three bolted steel-plate specimens were used in this experiment. For ease of identification, they are designated as B1, B2, and B3. All three specimens were fabricated from cold-rolled 16Mn steel plates of the same grade, and their manufacturing tolerances and surface roughness were controlled through machining and deburring processes performed on the same batch of material [36]. The same experimental conditions and steps were applied to all three samples, with the roles of each piezoelectric sheet remaining unchanged. An ultrasonic coupling agent was used between each magnetically attached piezoelectric ceramic sheet and the steel plate.

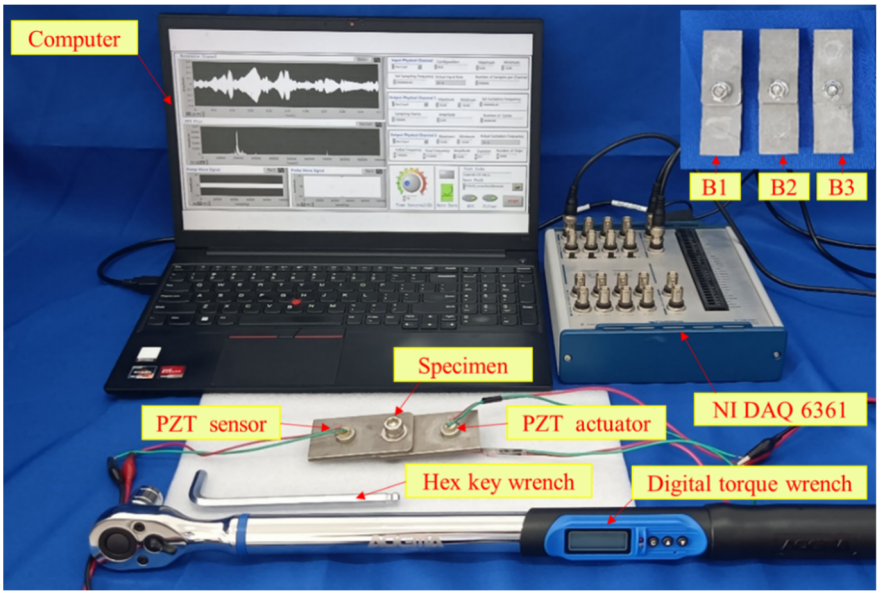



**Figure 3.** Experimental setup for VAM detection of bolted connections.

In this experiment, linear frequency-sweep signals and sine wave signals are emitted from the AO0 and AO1 ports of the NI DAQ 6361 data acquisition device, respectively. The AO0 port outputs a fixed-frequency sine wave excitation signal, while the AO1 port outputs a linear frequency-sweep excitation signal. Both signals act on the contact surface of the bolted steel plate, with the feedback signal collected by PZT3 on the opposite steel plate and input through the AI0 port to the NI DAQ 6361.

### *3.2. Experimental Process*

(1) To maximize the 'breathing' effect between the mating surfaces of rectangular steel plates connected by bolts, it is necessary to find the optimal parameters for the linear frequency-sweep signal. First, apply a wide-range linear frequency-sweep signal to the PZT1, starting at 60 kHz and ending at 250 kHz, with a sweep time of 0.1 s. Identify the peak point in the amplitude spectrum near 200 kHz. Consequently, determine the frequency range of the sweep signal to be 190–210 kHz.

(2) Apply a sweep signal to the pump signal excitation of PZT1, starting at 190 kHz and ending at 210 kHz, with a sweep time of 0.1 s, to induce breathing vibrations between the mating interfaces of the bolt connection. Apply a sinusoidal signal of 300 kHz to the detection signal excitation of PZT2. The two modulated vibration

(3) The bolt-tightening torque is applied using a digital torque wrench, ranging from 10 N·m to 30 N·m in 5 N·m increments. After each bolt torque load step is applied, the system is allowed to rest for 30 s to stabilize. Five consecutive vibration-acoustic signals pass through the bolt interface and are received by the piezoelectric sensor PZT3, sampled at a frequency of 2 MHz for a duration of 0.1 s.induced acoustic signals are then collected, and their average is taken as the representative signal for that load step. The signal is saved after passing through a high-pass filter (cutoff frequency of 100 kHz).

(4) Using the method described in Section 2.3, perform fractional Fourier filtering on the bolt connection vibro-acoustic modulation signal, ultimately obtaining an amplitude–frequency curve that includes both sum and difference frequency signal components.

## 4. Results and Discussion

The time-domain signal of the bolted joint vibration frequency modulation experiment is shown in Figure 4. From the local magnification of the time-domain signal, as shown in Figure 5, it can be seen that there is a clear modulation phenomenon in the received signal.

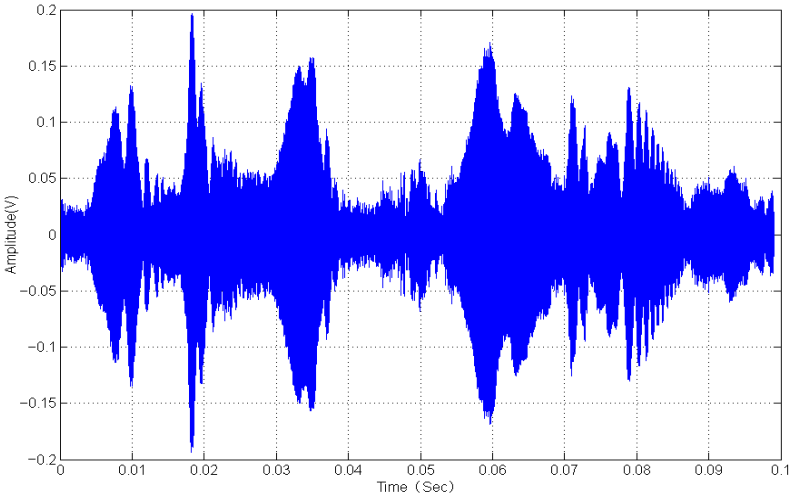



**Figure 4.** Time-domain signal diagram of bolted connection VAM experiment.

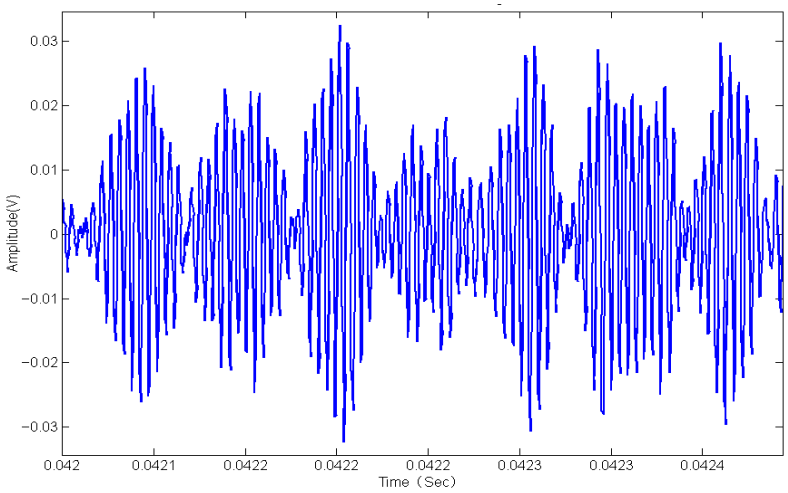



**Figure 5.** Enlarged view of the time-domain signal of the bolted connection VAM.

Calculate the signal energy value E for the time-domain signals received by sample B1 under different tightening torques using Formula (9).

$$E = \sum_{i=1}^{n} a_i^2 \tag{9}$$

From Figure 6, it can be seen that there is no obvious linear correlation between the time-domain signal energy and the bolt-tightening torque.

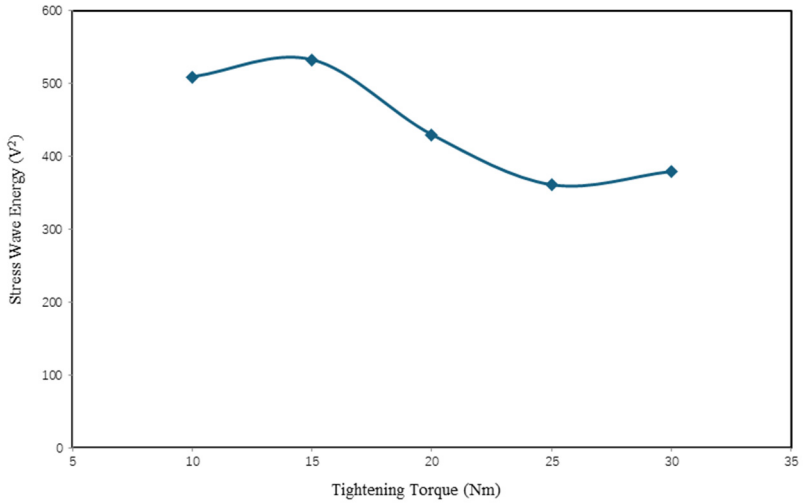



**Figure 6.** Signal time-domain energy corresponding to different tightening torques.

The Fourier transform of the signal yields its amplitude spectrum, as shown in Figure 7. The graph shows multiple peaks around the 200 kHz frequency, with distinct peaks at 300 kHz and 700 kHz. The 300 kHz peak corresponds to the detection sine signal frequency, while the 700 kHz peak represents the sum and difference frequency signals of the VAM. Linear frequency-sweep signals are used to create a 'breathing' effect on crack surfaces, and their signal energy is much stronger than that of sinusoidal detection signals. Therefore, using the FrFT to filter out the linear frequency-sweep signal components while retaining the sinusoidal and harmonic components can help improve the analysis accuracy of beat frequencies.

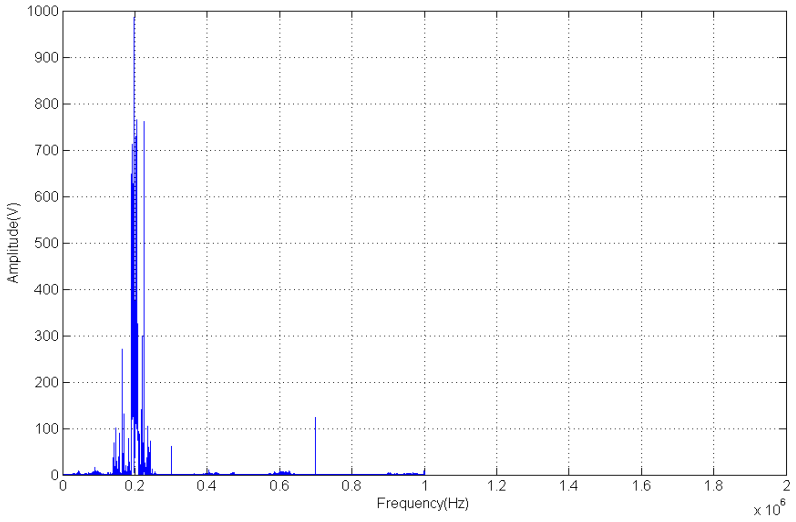



**Figure 7.** Amplitude–frequency diagram obtained after FFT of the VAM signal.

The received signal is transformed using FrFT. To improve computational efficiency, a coarse scan with large steps is first performed, followed by a fine scan with small steps to obtain the optimal fractional order FRFT. This paper uses a linear frequency-sweep signal starting at 190 kHz, ending at 210 kHz, and lasting 0.1 s, which shows significant concentration in the fractional domain, as shown in Figure 8.

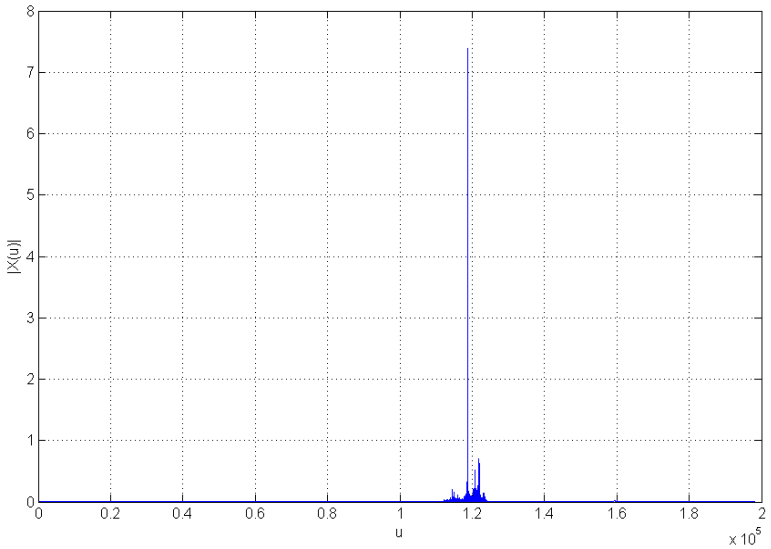



**Figure 8.** Optimal fractional-order domain amplitude plot of feedback signals.

Using the masking filtering method, for the u value corresponding to the peak point of the optimal fractional-order $p^*$ Fourier transform domain, within the range of $\pm 0.05$u, set its fractional-order domain amplitude to 0 for masking filtering. The filtering effect is shown in Figure 9. After removing the linear frequency-sweep signal, perform a $-p^*$ order transformation on the signal to obtain the time-domain signal, as shown in Figure 10. Comparing Figures 4 and 10 reveals that after removing the linear frequency-sweep signal, the amplitude of the time-domain signal significantly decreases.

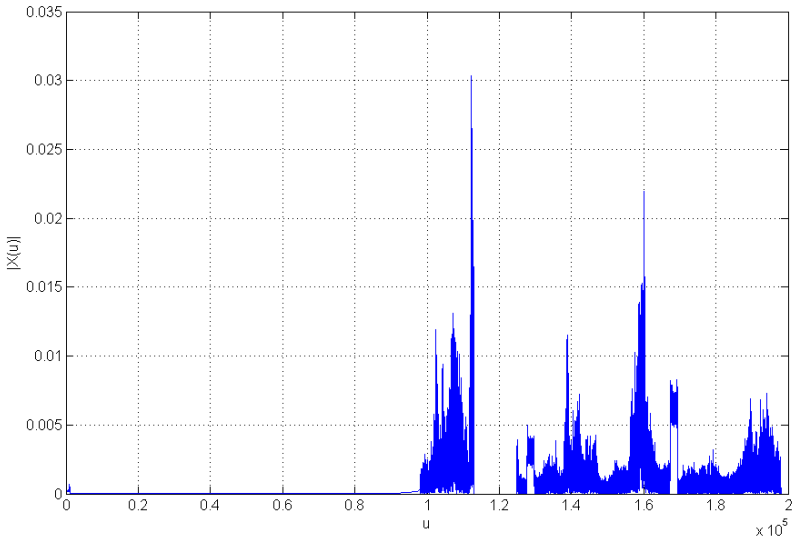



**Figure 9.** Optimal fractional domain plot after removing linear frequency-sweep signal.

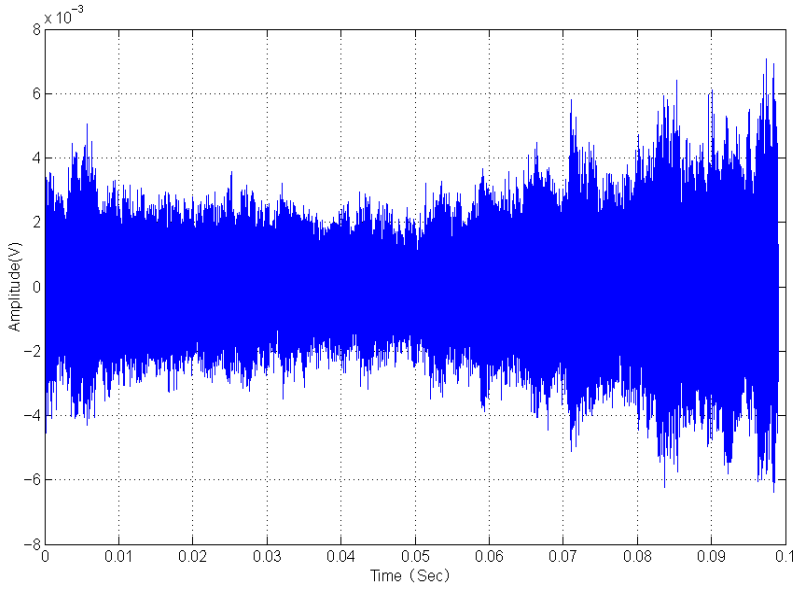



**Figure 10.** Time-domain plot of the signal after removing the linear frequency-sweep.

Finally, perform a Fourier transform on the time-domain signal to obtain the amplitude–frequency spectrum of the signal after removing the linear frequency-sweep signal, as shown in Figure 11. It can be observed that, within the range below 200 kHz, multiple harmonic signal peaks exist. In comparison, the amplitude of the 300 kHz sinusoidal detection signal and the 700 kHz beat frequency signal is relatively significant. Therefore, this study uses the amplitude of the 700 kHz beat frequency signal as an evaluation parameter for the degree of bolt loosening.

As the tightening torque increases from 10 N·m to 30 N·m, with increments of 5 N·m per load step, the amplitudes of the sum and difference frequency signals at 700 kHz in the frequency domain are shown in Figure 12. It can be observed from the figure that three sets of bolted joint specimens, B1, B2, and B3, have collected vibration acoustic modulation signals. After filtering with a linear frequency-sweep signal, the amplitude of the 700 kHz harmonic increases with the increase in tightening torque within the range of 10 N·m to 30 N·m. At a tightening torque of 10 N·m, due to the initial contact between the two steel plates, the state is relatively unstable, showing a more significant change compared to other conditions.

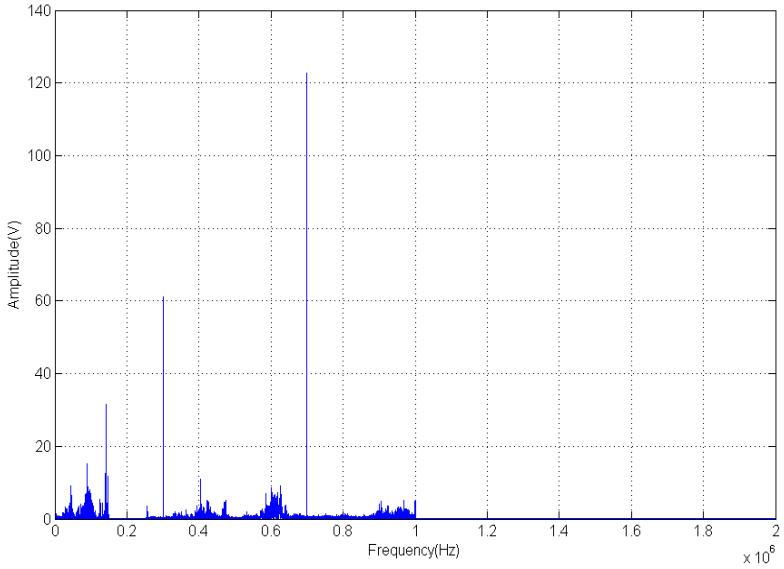



**Figure 11.** Spectrum amplitude plot of the signal after removing the linear frequency-sweep.

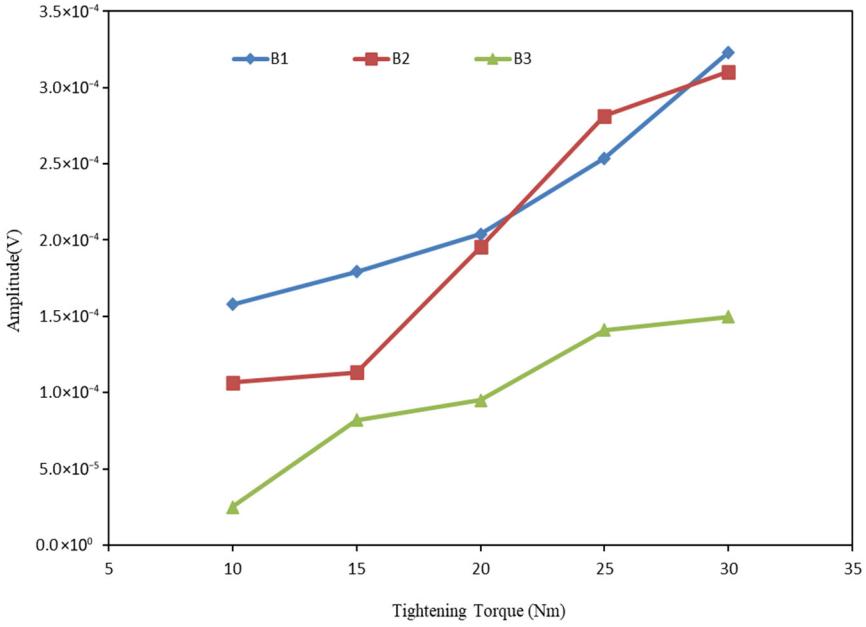



**Figure 12.** The relationship between bolt-tightening torque and the amplitude of the 700 kHz signal.

According to Hertz contact theory [37–39], the actual contact area of two steel plates bolted in this study increases with the increase in tightening torque. Under the vibration excitation of a low-frequency pump signal, the "breathing" effect between contact surfaces is enhanced, and the amplitude of nonlinear modulation response increases accordingly. The experimental results in this paper verify this rule as a whole and show that, by detecting the vibration acoustic modulation signal and adopting the proposed method, the looseness degree of bolt connection can be effectively evaluated according to the amplitude change in sum and difference frequency harmonics. It is worth noting that there is a certain difference in peak amplitude between sample B3, B1 and B2 in Figure 12, which may be due to slight inconsistency in the pasting of piezoelectric sheets or inherent material fluctuation between samples. Although the change trend of each sample is consistent, the above deviation still suggests that the influence of physical setting difference and manufacturing tolerance on the test results should be considered in engineering application.

## 5. Conclusions

In this paper, we propose a novel method for detecting loose bolt connections based on FrFT and vibro-acoustic modulation. Compared to traditional vibro-acoustic modulation methods, the proposed method employs linear frequency-sweep signals for vibration excitation and fixed-frequency sinusoidal waves for high-frequency ultrasonic excitation. Additionally, in current vibro-acoustic modulation methods, using PZT transducers instead of vibrators enhances practicality in industrial applications. Subsequently, we introduce a new filtering method for vibro-acoustic modulation signals containing linear frequency-sweep signal components, based on the principle of the FrFT. Using the harmonic amplitudes obtained after signal-filtering, a damage index is proposed to estimate the relationship between tightening torque and modulated signals. Experimental results demonstrate that this new damage index exhibits a one-to-one correspondence with the bolt-tightening torque during the early stages of loosening. Therefore, we prove that the proposed vibro-acoustic modulation method has the capability to detect bolt loosening. The primary advantage of this method is its simplicity and robustness, making it reliable for detecting the degree of loosening in bolted connections.

**Author Contributions:** Conceptualization, X.W., N.L. and Q.J.; methodology, H.Y.; software, J.Q.; validation, H.Z.; formal analysis, N.Z.; investigation, Q.J.; resources, X.W., H.Y. and J.Q.; data curation, X.W.; writing—original draft preparation, X.W., N.L. and Q.J.; writing—review and editing, X.W., H.Z. and N.Z.; visualization, X.W. and Q.J.; supervision, X.W. and Q.J.; project administration, X.W., Q.J. and H.Z.; funding acquisition, X.W. and H.Z. All authors have read and agreed to the published version of the manuscript.

**Funding:** This research was funded by Open Fund of State Key Laboratory of Oil and Gas Reservoir Geology and Exploitation (Southwest Petroleum University), China under Grant PLN2022-26.

**Data Availability Statement:** The original contributions presented in this study are included in the article. Further inquiries can be directed to the corresponding authors.

**Acknowledgments:** The authors would like to thank the anonymous reviewers for their valuable comments and suggestions that helped improve the quality of this paper.

**Conflicts of Interest:** Authors Xiaogang Wang, Hai Yang, Jingjing Qi, Hao Zhang, and Ning Zhao were employed by the Sinopec (Shandong) Test, Evaluation & Research Co., Ltd. and Shengli Oilfield Branch Technical Testing Center. The remaining authors declare that the research was conducted in the absence of any commercial or financial relationships that could be construed as a potential conflict of interest. The Sinopec (Shandong) Test, Evaluation & Research Co., Ltd. and Shengli Oilfield Branch Technical Testing Center had no role in the design of the study; in the collection, analyses, or interpretation of data; in the writing of the manuscript, or in the decision to publish the results.

## Abbreviations

The following abbreviations are used in this manuscript:

| | |
|---|---|
| VAM | Vibro-Acoustic Modulation |
| LFM | Linear Frequency Modulation |
| FrFT | Fractional Fourier Transform |

## References

1. Huang, J.; Liu, J.; Gong, H.; Deng, X. A comprehensive review of loosening detection methods for threaded fasteners. *Mech. Syst. Signal Process.* **2022**, *168*, 108652. [CrossRef]
2. Miao, R.; Shen, R.; Zhang, S.; Xue, S. A review of bolt tightening force measurement and loosening detection. *Sensors* **2020**, *20*, 3165. [CrossRef] [PubMed]
3. Jia, J.; Hu, H.; Tao, L.; Yang, D. Analysis of load effect on nonlinear vibro-acoustic modulation used in on-line monitoring of fatigue cracks. *Smart Mater. Struct.* **2017**, *26*, 095048. [CrossRef]

4. Nguyen, H.; Zhu, R.; Chen, J.K.; Tracy, S.L.; Huang, G.L. Analytical coupled modeling of a magneto-based acoustic metamaterial harvester. *Smart Mater. Struct.* **2018**, *27*, 055010. [CrossRef]
5. Wang, F. Identification of multi-bolt head corrosion using linear and nonlinear shapelet-based acousto-ultrasonic methods. *Smart Mater. Struct.* **2021**, *30*, 085031. [CrossRef]
6. Yuan, R.; Lv, Y.; Xu, S.; Li, L.; Kong, Q.; Song, G. ResNet-integrated very early bolt looseness monitoring based on intrinsic feature extraction of percussion sounds. *Smart Mater. Struct.* **2023**, *32*, 034002. [CrossRef]
7. Zhao, N.; Huo, L.; Song, G. Vibration acoustic modulation for bolt looseness monitoring based on frequency-swept excitation and bispectrum. *Smart Mater. Struct.* **2023**, *32*, 034004. [CrossRef]
8. Song, G.B.; Li, W.J.; Wang, B.; Ho, S.C.M. A Review of Rock Bolt Monitoring Using Smart Sensors. *Sensors* **2017**, *17*, 776. [CrossRef]
9. Li, D.; Nie, J.-H.; Wang, H.; Ren, W.-X. Loading condition monitoring of high-strength bolt connections based on physics-guided deep learning of acoustic emission data. *Mech. Syst. Signal Process.* **2024**, *206*, 110908. [CrossRef]
10. Li, N.; Wang, F.; Song, G. Monitoring of bolt looseness using piezoelectric transducers: Three-dimensional numerical modeling with experimental verification. *J. Intell. Mater. Syst. Struct.* **2020**, *31*, 911–918. [CrossRef]
11. Du, F.; Wu, S.W.; Xing, S.S.; Xu, C.; Su, Z. Temperature compensation to guided wave-based monitoring of bolt loosening using an attention-based multi-task network. *Struct. Health Monit.* **2023**, *22*, 1893–1910. [CrossRef]
12. Sui, X.D.; Duan, Y.F.; Yun, C.; Tang, Z.; Chen, J.; Shi, D.; Hu, G. Bolt looseness detection and localization using wave energy transmission ratios and neural network technique. *J. Infrastruct. Intell. Resil.* **2023**, *2*, 100025. [CrossRef]
13. Wang, F.R.; Chen, Z.; Song, G.B. Monitoring of multibolt connection looseness using entropy-based active sensing and genetic algorithm-based least square support vector machine. *Mech. Syst. Signal Process.* **2020**, *136*, 106507. [CrossRef]
14. Chen, L.; Xiong, H.; Yang, Z.; Long, Y.; Ding, Y.; Kong, Q. Preload measurement of steel-to-timber bolted joint using piezoceramic-based electromechanical impedance method. *Measurement* **2022**, *190*, 110725. [CrossRef]
15. Fan, J.; Chen, W.; Chen, D.; Chen, H.; Luo, L.; Bao, S. Vibro-acoustic modulation-based bolt looseness detection method using frequency sweep probe waves. *Nondestruct. Test. Eval.* **2023**, *39*, 1147–1168. [CrossRef]
16. Gao, X.; Wang, W.; Du, J. Bolt load looseness detection for slip-critical blind bolt based on wavelet analysis and deep learning. *Structures* **2024**, *64*, 106521. [CrossRef]
17. Huo, L.S.; Wang, F.R.; Li, H.N.; Song, G. A fractal contact theory based model for bolted connection looseness monitoring using piezoceramic transducers. *Smart Mater. Struct.* **2017**, *26*, 9. [CrossRef]
18. Jiang, T.; Li, Y.; Song, G. Detection of High-Strength Bolts Looseness Using Lead Zirconate Titanate Due to Wavelet Packet Analysis. In *Earth and Space 2018: Engineering for Extreme Environments*; American Society of Civil Engineers: Reston, VA, USA, 2018; pp. 1069–1077. [CrossRef]
19. Kong, Q.; Zhu, J.; Ho, S.C.M.; Song, G. Tapping and listening: A new approach to bolt looseness monitoring. *Smart Mater. Struct.* **2018**, *27*, 07LT2. [CrossRef]
20. Qin, X.; Peng, C.; Zhao, G.; Ju, Z.; Lv, S.; Jiang, M.; Sui, Q.; Jia, L. Full life-cycle monitoring and earlier warning for bolt joint loosening using modified vibro-acoustic modulation. *Mech. Syst. Signal Process.* **2022**, *162*, 108054. [CrossRef]
21. Nguyen, T.T.; Tuong Vy Phan, T.; Ho, D.D.; Pradhan, A.M.S.; Huynh, T.C. Deep learning-basedautonomousdamage-sensitivefeatureex-tractionforimpedance-basedprestress monitoring. *Eng. Struct.* **2022**, *259*, 114172. [CrossRef]
22. Yin, H.Y.; Wang, T.; Yang, D.; Liu, S.; Shao, J.; Li, Y. A Smart Washer for Bolt Looseness Monitoring Based on Piezoelectric Active Sensing Method. *Appl. Sci.* **2016**, *6*, 320. [CrossRef]
23. Zhou, Y.; Yi, H.; Yue, X.; Li, A.; Hao, B.; Yan, X.; Zhao, Y. Method for loose bolt positioning and prediction of bolt axial force in bolt group. *Measurement* **2024**, *227*, 114316. [CrossRef]
24. Du, G.; Kong, Q.; Lai, T.; Song, G. Feasibility study on crack detection of pipelines using piezoceramic transducers. *Int. J. Distrib. Sens. Netw.* **2013**, *9*, 631715. [CrossRef]
25. Wang, F.; Chen, Z.; Song, G. Smart crawfish: A concept of underwater multi-bolt looseness identification using entropy-enhanced active sensing and ensemble learning. *Mech. Syst. Signal Process.* **2021**, *149*, 107186. [CrossRef]
26. Li, J.; Wen, B.; Zhang, Z.; Li, Q.; He, Y.; Su, Z. Interface behaviors of elastic-plastic waves and its impact on uncertainties in vibro-acoustic modulation (VAM) for structural health monitoring (SHM) of bolt loosening. *Mech. Syst. Signal Process.* **2024**, *212*, 111268. [CrossRef]
27. Wang, F.; Song, G. Bolt early looseness monitoring using modified vibro-acoustic modulation by time-reversal. *Mech. Syst. Signal Process.* **2019**, *130*, 349–360. [CrossRef]
28. Li, N.; Wang, F.R.; Song, G.B. New entropy-based vibro-acoustic modulation method for metal fatigue crack detection: An exploratory study. *Measurement* **2020**, *150*, 9. [CrossRef]
29. Parsons, Z.; Staszewski, W.J. Nonlinear acoustics with low-profile piezoceramic excitation for crack detection in metallic structures. *Smart Mater. Struct.* **2006**, *15*, 1110–1118. [CrossRef]
30. Zhao, N.; Huo, L.; Song, G. A nonlinear ultrasonic method for real-time bolt looseness monitoring using PZT transducer–enabled vibro-acoustic modulation. *J. Intell. Mater. Syst. Struct.* **2020**, *31*, 364–376. [CrossRef]

31. Wang, F.; Song, G. Monitoring of multi-bolt connection looseness using a novel vibro-acoustic method. *Nonlinear Dyn.* **2020**, *100*, 243–254. [CrossRef]
32. Namias, V. The fractional order Fourier transform and its application to quantum mechanics. *IMA J. Appl. Math.* **1980**, *25*, 241–265. [CrossRef]
33. Liu, D.; Qu, H.; Wang, W.; Deng, J. Multiple Targets Detection of Linear Frequency-Modulated Continuous Wave Active Sonar Using Fractional Fourier Transform. *Integr. Ferroelectr.* **2020**, *209*, 1–10. [CrossRef]
34. Gomez-Echavarria, A.; Ugarte, J.P.; Tobon, C. The fractional Fourier transform as a biomedical signal and image processing tool: A review. *Biocybern. Biomed. Eng.* **2020**, *40*, 1081–1093. [CrossRef]
35. Yang, Y.; Peng, Z.; Zhang, W.; Meng, G. Parameterised time-frequency analysis methods and their engineering applications: A review of recent advances. *Mech. Syst. Signal Process.* **2019**, *119*, 182–221. [CrossRef]
36. Teloli, R.D.O.; Butaud, P.; Chevallier, G.; da Silva, S. Good practices for designing and experimental testing of dynamically excited jointed structures: The Orion beam. *Mech. Syst. Signal Process.* **2022**, *163*, 108172. [CrossRef]
37. Sejdić, E.; Djurović, I.; Stanković, L. Fractional Fourier transform as a signal processing tool: An overview of recent developments. *Signal Process.* **2011**, *91*, 1351–1369. [CrossRef]
38. Ozaktas, H.M.; Arikan, O.; Kutay, M.A.; Bozdagt, G. Digital computation of the fractional Fourier transform. *IEEE Trans. Signal Process.* **1996**, *44*, 2141–2150. [CrossRef]
39. Zhao, G.; Li, S.-X.; Xiong, Z.-L.; Gao, W.-D.; Han, Q.-K. A statistical model of elastic-plastic contact between rough surfaces. *Trans. Can. Soc. Mech. Eng.* **2018**, *43*, 38–46. [CrossRef]


**Disclaimer/Publisher's Note:** The statements, opinions and data contained in all publications are solely those of the individual author(s) and contributor(s) and not of MDPI and/or the editor(s). MDPI and/or the editor(s) disclaim responsibility for any injury to people or property resulting from any ideas, methods, instructions or products referred to in the content.